Journal Pre-proof

Synthesis, characterization and in vitro biocompatibility study of strontium titanate ceramic: A potential biomaterial

Souvik Sahoo, Arijit Sinha, Mitun Das

PII: S1751-6161(19)30951-8

DOI: https://doi.org/10.1016/j.jmbbm.2019.103494

Reference: JMBBM 103494

To appear in: *Journal of the Mechanical Behavior of Biomedical Materials*

Received Date: 8 July 2019

Revised Date: 13 October 2019

Accepted Date: 13 October 2019

Please cite this article as: Sahoo, S., Sinha, A., Das, M., Synthesis, characterization and in vitro biocompatibility study of strontium titanate ceramic: A potential biomaterial, *Journal of the Mechanical Behavior of Biomedical Materials* (2019), doi: https://doi.org/10.1016/j.jmbbm.2019.103494.

Synthesis, characterization and in vitro biocompatibility study of strontium titanate ceramic: A potential biomaterial

Souvik Sahoo[a,b], Arijit Sinha[a], Mitun Das[b,c,*]

[a]School of Materials Science and Engineering, Indian Institute of Engineering Science and Technology, Shibpur, Howrah-711103, India

[b]Bioceramics and Coating Division, CSIR-Central Glass & Ceramic Research Institute, 196 Raja S. C. Mullick Road, Kolkata-700032, India

[c]Biomaterials and Corrosion Lab, Department of Materials Science and Engineering, Tel-Aviv University, Ramat Aviv 6997801, Israel

[*]**Corresponding Author:** Dr. Mitun Das

E-mail: mitun@cgcri.res.in

Abstract

Strontium (Sr), a mineral element present in trace in the human body, has significant effect on bone remodelling. Sr containing ceramics have huge potential to heal bone defects and improve osseointegration of implants. In this study, perovskite oxide – strontium titanate ($SrTiO_3$) was synthesized and explored its potential for biomedical applications. The phase pure $SrTiO_3$ powder was synthesized from solid state reaction of strontium carbonate ($SrCO_3$) and titanium dioxide (TiO_2) at 1200 ºC for 2 h. The as synthesized $SrTiO_3$ powder, pure hydroxyapatite (HAp) and $SrTiO_3$-50 wt.% HAp (SH50) premixed powders were sintered at different temperatures varies from 1100 to 1400 ºC in air. The sintered samples were characterized using X-ray diffraction (XRD) for phases and scanning electron microscopy (SEM) for microstructure analysis. XRD results revealed no dissociation of HAp or reaction with $SrTiO_3$ during sintering. The sintered samples were studied for mechanical properties, wettability, and biocompatibility. The relative density of the sintered $SrTiO_3$ increases with increasing sintering temperature. The relative density of $SrTiO_3$ was increased from 77% to 98 % with increase in sintering temperature from 1250 to 1400 °C. The substantial improvement of hardness and compressive strength was observed for sintered $SrTiO_3$ compared to HAp of similar porosity level. The hardness and compressive strength of $SrTiO_3$ sintered at 1250 °C found ~6 and ~3.5 times higher than sintered HAp. In vitro dissolution study carried out in phosphate buffer solution at 37 °C, confirmed the release of Sr^{2+} ion from the bulk $SrTiO_3$ sintered at 1250 °C. The in vitro cell materials interaction showed cytocompatibility of sintered $SrTiO_3$ and $SrTiO_3$-HAp composite. In summary, excellent biocompatibility of $SrTiO_3$ with superior mechanical properties confirmed its potential as novel biomaterial for use in the repair of infected or aseptic bone defects.

Keywords: Strontium; Hydroxyapatite; Biocompatibility; Mechanical property; Nanoindentation,

1. Introduction

The development of new bone substitute material, with improved osteoconductivity, functionality and mechanical properties, is of great interest. Till now calcium phosphate based bioceramics, i.e. hydroxyapatite (HAp) and β-tricalcium phosphate (β-TCP) are the mostly used materials for tissue engineering and bone repairing, because of their chemical similarity with inorganic phase of bone, biocompatible and osteoconductivity [1,2]. However, calcium phosphate based ceramics exhibited low mechanical properties (brittleness and low strength) which limits its applications as an implant material [3,4]. Therefore, there is a need for alternative materials or combination of different materials to enhance mechanical properties of existing bioactive ceramics as well as slow release of essential ions to promote both osteogenesis and angiogenesis [5]. Several research efforts have been made in this direction for developing new resorbable bioceramics with improved mechanical properties for bone tissue engineering [5-8].

Strontium (Sr), alkaline earth metal, present in trace amount in human body that is 0.00044% of a standard 70 kg body mass [9]. Sr mostly present in the mineral phase of bone along with calcium owing to their chemical similarity and followed the metabolic pathways almost similar to calcium [10,11]. Since 2004 Sr has got huge clinical interest due to the development of strontium ranelate (SrRan) – a very useful drug for treatment of postmenopausal osteoporosis [12]. SrRan prevents bone loss by enhancing differentiation of pre-osteoblastic cells and inhibit the osteoclastic cells formation [13]. Different types of vertebral, peripheral and hip fracture of the bone decrease due to oral administration of SrRan within the patients [12,14]. In view of promising effects of Sr on bone, several studies were performed to evaluate effect of strontium incorporation, in calcium phosphate and calcium-silica based synthetic materials – in terms of crystal structure, stability, mechanical

behaviour, in vitro and in vivo performance. Recent studies on Sr incorporated calcium-silica based ceramics showed superior bone regeneration and angiogenesis in a critical sized calvarial defect model, in comparison with pure calcium-silica bioceramic [5,15]. Huang et al. showed that the degradation rate of calcium silicate cements increased with increasing strontium content in the cements [16]. The improved degradation raised the ionic products in the microenvironment which stimulate the angiogenic and osteogenic differentiation. Further, the studies have shown that increasing substitution of calcium in HAp by Sr ion can apparently decrease thermal stability and increase the solubility of the material [17,18]. In addition, Sr substituted HAp and bioglass in the form of powders, granules, porous scaffolds, and bioactive coatings showed a superior bone regeneration capability than the pure synthetic materials [19-23]. In vitro studies showed the attachment and proliferation of osteoblast cells by addition of Sr in HAp [21]. Sr has a significant effect in reducing osteoporosis of the bones by inhibition of osteoclastogenesis and stimulate osteoblast cells for regeneration of bone [21,22]. However, there is not much literature available to explore the potential of Sr based compounds as biomaterial. There are few literatures available where Sr based compounds such as strontianite ($SrCO_3$) and strontium titanate ($SrTiO_3$) nanotubes were used as coating materials for sustained release of Sr [14, 24-29]. Our previous study on laser deposition of $SrTiO_3$ reinforced Ti matrix coatings showed sustain release of Sr^{2+} from Ti surface which effectively enhanced cell viability of surface modified Ti [27]. Strontium titanate, a perovskite oxide, has wide range of applications as piezoelectric, photocatalytic and electronic devices [30, 31]. Due to its interesting functional properties, not much attention has been given on structural and biocompatible aspect of the bulk ceramic. Therefore, in this study we focused on synthesis, sintering of $SrTiO_3$ at different temperatures, in vitro degradation behaviour and in vitro cellular interactions using mouse embryonic fibroblast (NIH3T3) cell line, to understand its potential in biomedical

applications. Further, mechanical behaviour in micro and nanoscale, and wettability of sintered $SrTiO_3$ were compared with sintered HAp.

2. Materials and Methods

2.1 Powder synthesis

In the present work, strontium carbonate ($SrCO_3$, Sigma-Aldrich) and titanium dioxide (TiO_2, Sigma-Aldrich) powder were used to produce strontium titanate ($SrTiO_3$) by solid state reaction. $SrCO_3$ and TiO_2 powders in stoichiometry were ball-milled in a zirconia vial in ethyl alcohol medium for 8 h. The mixed powders were dried in a hot oven followed by calcination at 1200 °C for 2 h. The calcined powders were ground and sieved to get fine $SrTiO_3$ powder. Further, a fraction of calcined $SrTiO_3$ powders were mixed with 50 wt.% HAp powders (Merck, Germany) using wet ball milling for 8 h to develop homogeneous mixing of powders which was further used for composite preparation.

2.2 Sintering of ceramic

The fine powders of $SrTiO_3$ (calcined), commercial HAp and premixed $SrTiO_3$-50HAp powders were mixed with 2% polyvinyl alcohol (PVA) solution, followed by uniaxially pressed in a 15 mm die. The green pellets were cold isostatically pressed (CIP; EPSI, Walgoedstraat, Belgium) at 150 MPa pressure. The HAp and the $SrTiO_3$-50HAp green pellets were sintered at 1100 °C for 1 h to restrain any dissociation of HAp phase. The $SrTiO_3$ green compacts were sintered at different temperatures varies from 1250 to 1400 °C for 2 h. Density of the sintered samples were measured using Archimedes principle. The relative density of the sintered specimens was measured by taking the theoretical density of the $SrTiO_3$ and HAp as 5.12g/cm^3 [32] and 3.16 g/cm^3 [33], respectively. The theoretical density

of the $SrTiO_3$-50HAp composite was calculated as 4.13 g/cm^3 from the rule of mixture. The sample nomenclature as well as compositions and sintering temperatures are summarized in Table 1.

Table 1. Density and crystallite size measurement for the bulk sintered specimens.

Specimen ID	Composition	Sintering temperature (°C)	Actual density (g/cm^3)	Relative density (%)	Crystallite size (nm)
HAp	Pure HAp	1100	2.12	67	41
SH50	HAp-50$SrTiO_3$	1100	2.55	62	42 (HAp) 49 ($SrTiO_3$)
ST1250	Pure $SrTiO_3$	1250	3.92	77	45
ST1350	Pure $SrTiO_3$	1350	4.50	88	47
ST1400	Pure $SrTiO_3$	1400	5.03	98	49

2.3 Phase analysis

X-ray diffraction (XRD) analysis was carried out using X'Pert Pro MPD diffractometer (Panalytical, Almelo, Netherlands) in the range of 20º to 80º for the as synthesized powder and sintered specimens. The crystallite size of the sintered specimens was determined using Scherrer equation.

$$d = \frac{k \cdot \lambda}{\beta \cdot cos\theta} \quad (1)$$

Where d = crystallite size (nm), k = shape factor (0.9 by assuming spherical crystallite), β = full width half maximum (FWHM) of the highly intense (110) $SrTiO_3$ peak and (211) HAp peak, θ = Bragg angle.

The microstructure of the sintered samples was carried out using Field emission scanning electron microscopy (FESEM; Zeiss, Jena, Germany). Before FESEM, samples were sputter coated with gold (Au) to make the samples conductive.

2.4 Mechanical behaviour study

The hardness of the sintered specimens was measured at micro as well as nano scale range. Before hardness measurement, the specimens were polished upto 1 µm diamond paste. Vicker's micro-hardness (ESEWAY, Camberley, United Kingdom) measurement for all the sintered ceramic samples was carried out at different loads (100, 200, 300 and 500 g) for 15 sec dwell time and an average of five measurements were reported. Total nine indentations (3×3 matrix) for each specimen at a maximum load of 8 mN applied by nano-indentation (Hysitron, Minneapolis, USA) technique. Loading, dwell and unloading time for each indentation were 10-10-10 sec, respectively. The hardness and reduced elastic modulus of the sintered materials were measured from load-depth curve using Oliver-Pharr method.

The compressive strength of the cylindrical sintered samples was measured based on ASTM C773 standard. The dimensions of the sintered $SrTiO_3$ and HAp samples used for compressive strength measurement were 7 mm in diameter and 12.6 mm in height. The crosshead speed of 1mm/min was used for all the specimens.

2.5 Contact angle measurement

The wettability of the sintered ceramics was measured by the sessile drop method using drop shape testing machine (DSA25E, KRÜSS GmbH, Germany). Before the experiment, all the samples were polished upto 1 µm diamond paste, followed by ultrasonic cleaning in alcohol and dried in a hot oven at 100°C. The distilled water droplet size 5 µl and the flow rate 100 µl/min were used during the contact angle measurement. The water droplet dispensed over the sample surface and contact angle was measured from the droplet geometry by fitting curves. Total 10 droplets were taken to measure the average contact angle for each type of specimen.

2.6 Dissolution behaviour

The dissolution behaviour of sintered sample (ST1250) was studied in the phosphate buffered saline (PBS, Sigma) solution. The ST1250 was put into the PBS solution at a concentration of 0.1 gm solid in 30 ml solution and kept it in the incubator at 37°C for 7, 14 and 21 days. After filtration, the extracted solution was used for ion release (Sr^{2+} and Ti^{2+} ion) study using inductively coupled plasma analytical technique (ICP; Spectra Analytical Instrument GmbH, Kleve, Germany).

2.7 Bioactivity study

In vitro cell culture was performed for the sintered ceramic specimens, namely HAp, SH50 and ST1250, of identical dimensions (Ø 12mm) and surface roughness. All the polished samples were cleaned in a sonicator using distilled water followed by ethyl alcohol and then sterilized in an autoclave at 121°C for 30 min. Biocompatibility of the materials was evaluated using mouse embryonic fibroblast cell line (NIH3T3, NCCS Pune, India). The NIH3T3 cell lines were cultured in Dulbecco's Minimum Essential Medium (DMEM, Gibco), supplemented with 10% foetal bovine serum (FBS, Sigma) and 1% antibiotic-antimycotic solution (50 $\mu g \cdot mL^{-1}$streptomycin and 50 $\mu g \cdot mL^{-1}$ gentamycin, Sigma) at 37 °C in the atmosphere of 5% CO_2. The confluent cells were removed from T75 flask and a cell suspension prepared. In a sterile hood, samples were transferred in a 24 well plate and cell suspension containing 5×10^4 cells were seeded on the sample surface. The cells were cultured on the sample surface for 2, 4 and 6 days. After each time period, samples in triplet were used for MTT assay to evaluate cell viability and proliferation. Details of the MTT protocol can be seen elsewhere [34]. Statistical analysis was performed on the data using Student's t-test and $P < 0.05$ was considered statistically significant.

3. Results and discussion

3.1 Phase analysis

Fig. 1 shows the X-ray diffraction patterns of initial powders used for sintering and samples after sintering. The XRD of HAp powder and $SrTiO_3$ powder shown in **Fig. 1(a)**, revealed that the powder containing pure hydroxyapatite and strontium titanate phase, respectively. The $SrTiO_3$ powders were synthesized by calcination of premixed powders, $SrCO_3$ and TiO_2, at 1200°C. The solid state reactions occurred as follows:

$$SrCO_3 \rightarrow SrO + CO_2 \quad (2)$$

$$SrO + TiO_2 \xrightarrow{calcination} SrTiO_3 \quad (3)$$

XRD result of the calcined powder confirmed the absence of unreacted phases, indicating successful synthesis of phase pure $SrTiO_3$ powder. Further, the XRD patterns of the sintered HAp, HAp-50$SrTiO_3$ (SH50) and $SrTiO_3$ sintered at different temperatures (ST1250 and ST1400) were presented in **Fig. 1(b)**. The sintered HAp and SH50 samples showed major peaks correspond to HAp and $SrTiO_3$. It is clear from the results that after sintering at 1100°C, no dissociation of HAp was observed and no reaction occurred between HAp and $SrTiO_3$ in SH50 sample. Further, the $SrTiO_3$ samples sintered at various temperatures showed no trace of dissociated phases. **Table 1** shows the crystallite size of the sintered samples. There is no significant change in crystallite size was observed in $SrTiO_3$ specimens with increasing sintering temperature.

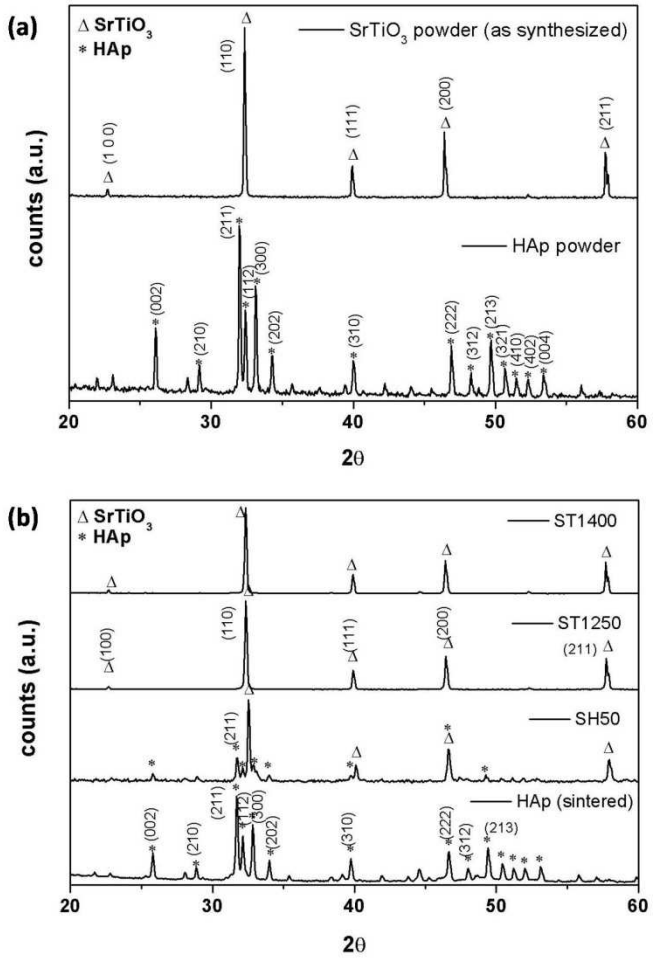

Figure 1. XRD patterns of (a) HAp and as synthesized $SrTiO_3$ powder, (b) sintered samples.

3.2 Sintered density and microstructure

The actual and relative densities of all the sintered specimens are presented in **Table 1**. The sintered HAp and SH50 samples were prepared from commercial HAp powders, showed significantly lower sintered density. Similarly, low sintered density was also observed in $SrTiO_3$ samples sintered at 1250°C. The relative sintered density of $SrTiO_3$ samples increased from 77% to 98% with increasing sintering temperature varies from 1250°C to 1400°C. The densification rate of $SrTiO_3$ has improved significantly by increasing sintering temperature from 1350°C to 1400°C. Higher sintering temperature promotes mass transport phenomenon by grain boundary and lattice diffusion at the inter-particle contact region. Thus decreases the

surface energy and enhances the relative density. However, to avoid any dissociation of HAp into β-TCP, sintering temperature of HAp and SH50 was kept at 1100 °C. Low sintering temperature and use of binder during compaction resulted porosity in the rage of 25 – 35% in HAp, SH50 and ST1250 samples. These porosities in the sintered specimens significantly reduce mechanical properties, even though porosity is essential for cell ingrowth.

The SEM micrographs of the sintered HAp, SH50, ST1250, ST1350 and ST1400 are shown in **Fig. 2**. A large number of pores can be observed in HAp, SH50 and ST1250 samples, sintered at low temperatures. The number of pores and pore size decreased with increasing sintering temperature from 1250°C to 1400 °C for $SrTiO_3$ specimen. Due to diffusion, the necking between neighbouring particles increases, pores gradually decrease and become spherical with increasing sintering temperature. The number of large size pores decreased with increasing sintering temperature.

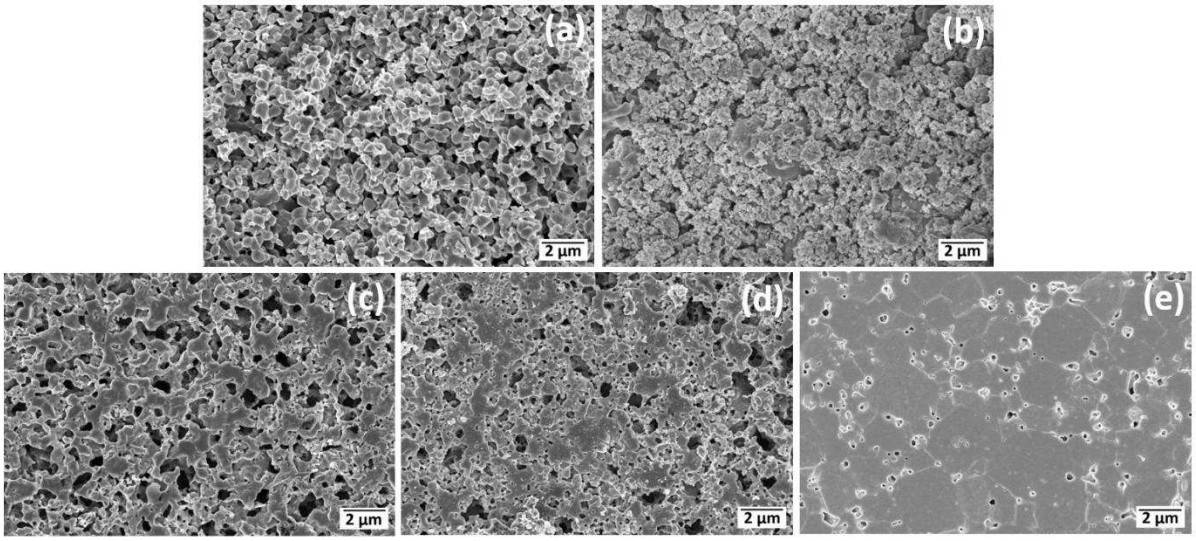

Figure 2. Scanning electron micrograph of sintered specimens (a) HAp sintered at 1100 °C, (b) SH50 sintered at 1100 °C, (c) ST1250 sintered at 1250 °C, (d) ST1350 sintered at 1350 °C, and (e) ST1400 sintered at 1400 °C.

3.3 Mechanical behaviour study

Fig. 3 shows the Vickers micro-hardness of sintered samples at different loads varies from 100 to 500 g. The average micro-hardness values of HAp, SH50, ST1250, ST1350 and ST1400 were 0.8, 0.9, 4.7, 5.9 and 8.1 GPa, respectively under the normal load of 100 g. There was no significant hardness improvement observed in SH50 samples compare to HAp. This may be due to lower sintering density of SH50 than HAp. It is clear from microhardness results that all the sintered $SrTiO_3$ samples showed superior hardness compared to sintered HAp and SH50 samples. The hardness of sintered $SrTiO_3$ increased gradually with sintering temperature. The significant hardness improvement was observed in ST1400 samples compare to ST1250. The high hardness in ST1400 is due to improve sintering density. Further, with increasing indentation loads, hardness values decreased for all the samples. The indentation size effect (ISE) is the main reason behind the hardness value reduction with increasing load.

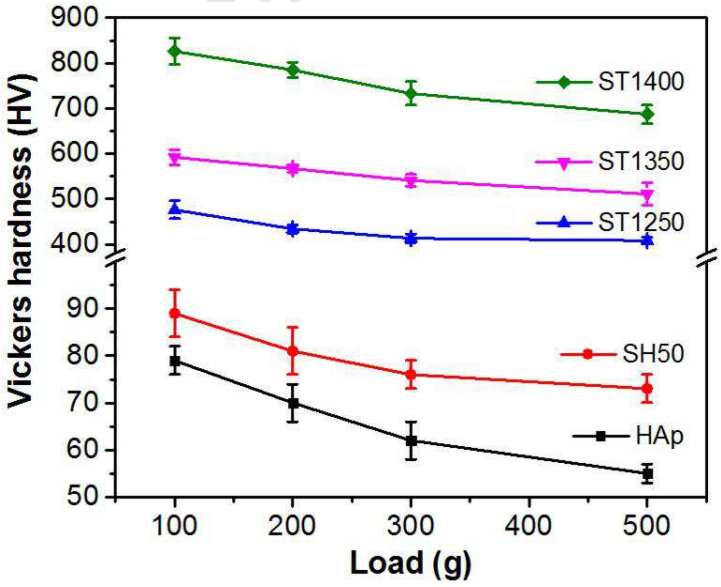

Figure 3. Vickers micro-hardness of sintered HAp, SH50, ST1250, ST1350 and ST1400 specimens.

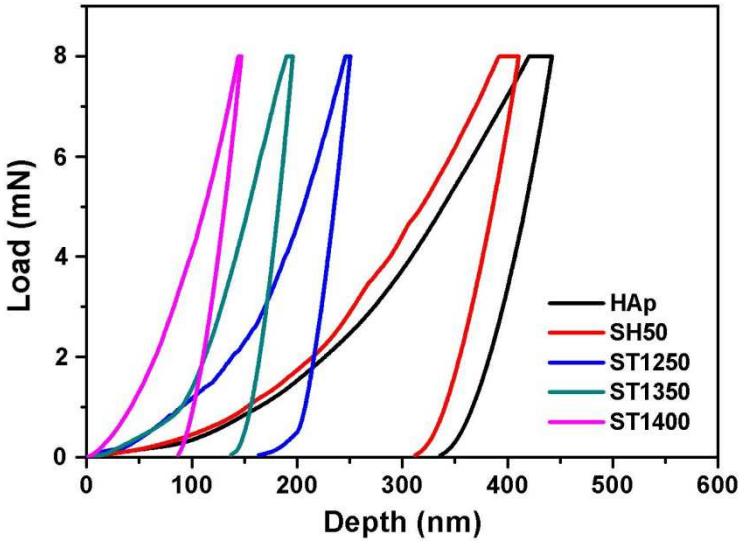

Figure 4. Nano-indention of the bulk sintered HAp, SH50, ST1250, ST1350 and ST1400 specimens.

The load-displacement curves from nanoindentation on the sintered samples carried out at a load of 8 mN and dwell time 10 s, are shown in **Fig. 4**. The depth of penetration and stiffness of the curves varies significantly for HAp, SH50, ST1250, ST1350 and ST1400. The results clearly showed that hardness and stiffness of the sintered samples are significantly different. **Table 2** summarises the hardness and reduced elastic modulus of sintered specimens obtained from nano-indentation. The hardness as well as reduced elastic modulus, become higher for sintered $SrTiO_3$ samples compared to HAp and SH50 specimen. The experimental data showed that average modulus increased from 153 ± 19 GPa in ST1250 to 248 ± 9 GPa for ST1400. In general, the modulus of elasticity and hardness of ceramics depend on the type of atomic bonding and the atomic arrangement. The $SrTiO_3$ has cubic perovskite structure with mixed ionic-covalent bondings. However, the mechanical properties of $SrTiO_3$ are not studied widely. Sakhya et al. recently reported the Young's modulus of $SrTiO_3$ as 277 GPa from first principales calculations using density functional theory [35]. In another report showed modulus of $SrTiO_3$ single crystal as 225 ±14 GPa, measured from nanoindentation [36]. The

hardness and modulus of $SrTiO_3$ sintered at 1400 °C found to be within the reported values. Moreover, improvement in density with increasing sintering temperature is the primary reason behind the gradual enhancement of hardness and elastic modulus of sintered $SrTiO_3$ samples.

Further, compressive strength of HAp, and ST1250 was compared because of their nearly similar pore fraction. The **Table 2** shows the compressive strength value of ST1250 and HAp specimens. The compressive strength of $SrTiO_3$ samples found much higher than HAp samples. The slightly high relative density of $SrTiO_3$ compared to HAp may be one of the reasons. However, bonding nature and crystal structure of $SrTiO_3$ is the reason behind large compressive strength value of bulk $SrTiO_3$. Nakamura et al. observed excellent plasticity in $SrTiO_3$ crystals when chemical composition in the crystal is properly controlled [37].The compressive strength of ST1250 becomes higher than the compressive strength of cortical bone (88.3-163.8 MPa), dentine (295 MPa), but, slightly lesser than the compressive strength of enamel (384 MPa) [30]. Therefore, $SrTiO_3$ could be a potential material for load bearing scaffolds.

Table 2. Hardness, reduced elastic modulus, compressive strength and contact angle of sintered ceramics

Specimen	**Hardness (H), (GPa)**	**Reduced elastic modulus (E_r), (GPa)**	**Compressive strength (MPa)**	**Contact angle (°)**
HAp	1.6 ± 0.5	46 ± 10	89 ± 11	82 ± 9
SH50	1.5 ± 0.3	54 ± 4	_	71 ± 8
ST1250	6.2 ± 1.8	153 ± 19	349 ± 70	59 ± 6
ST1350	9.5 ± 2.2	202 ± 12	_	-
ST1400	15.0 ± 1.2	248 ± 9	_	-

3.4 Dissolution and wettability study

The contact angles measured by the distilled water droplet on the polished surface of the sintered HAp, SH50 and ST1250 are presented in **Table 2**. The smaller contact angle on the bulk $SrTiO_3$ ceramic indicates more wettability than the HAp and SH50 materials. The wettable surface is desirable in biological environment that can enhance the protein absorption on the surface [34,38]. The hydrophilic nature of the surface also affects the dissolution of ion from the bulk. The dissolution behaviour of ST1250 was carried out in phosphate buffer solution (PBS) at a concentration of 0.1 gm solid in 30 ml solution. The concentration of Sr^{2+} and Ti^{2+} ions in PBS solution was measured after 7, 14 and 21 days through ICP analysis. ICP result revealed presence of Sr^{2+} ion in the filtered solution and no Ti^{2+} ions was detected. Xin et al. [25] mentioned the dissolution of the Sr^{2+} ion from $SrTiO_3$ as follows

$$SrTiO_3 + H_2O \rightarrow Sr^{2+} + TiO_2 + OH^-$$

Several researchers reported that the positive effect of Sr on osteoblastic cell responses [14, 24-27]. The release of Sr^{2+} in vivo is desirable which can significantly enhance preosteoblastic cell differentiation, proliferation and suppress osteoclast differentiation.

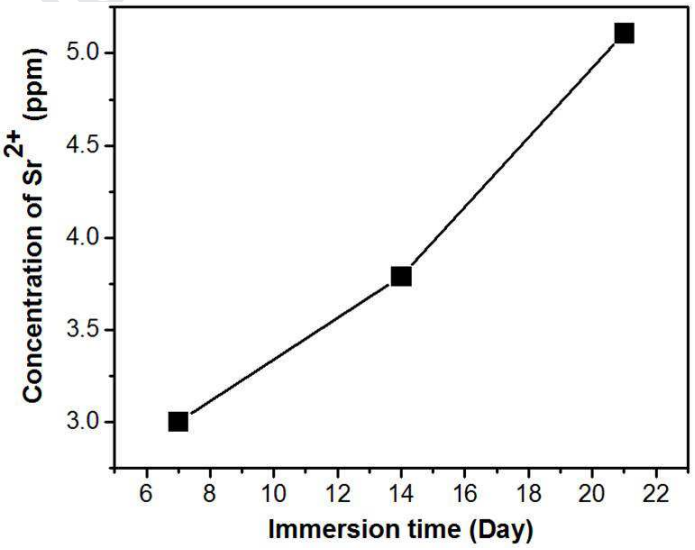

Figure 5. Sr^{2+} ion released from ST1250 specimen for different immersion times at the concentration of 0.1g solid per 30 ml PBS solution.

3.5 In vitro cell-material interactions

In vitro cytocompatibility of the sintered HAp, SH50, ST1250 samples were evaluated in presence of NIH3T3 using MTT assay for 2, 4 and 6 days. MTT assay measured the optical density which is equivalent to the number of living cells on the sample surface. Titanium samples were used as control. **Fig6** shows the optical density values for the samples at different time periods. The MTT assay clearly revealed that number of living cells on the ceramic samples increased with time. The content of living cells found significantly higher on HAp samples for all the culture duration. The metabolically active cells fibroblast cells on ST1250 and SH50 was significantly higher than Ti surface. The MTT results showed that the non-cytotoxic behaviour of the ST1250. The release of the Sr^{2+} ion from $SrTiO_3$ enhances the bioactivity $SrTiO_3$ and the bioactivity becomes higher than Ti for all the culture time.

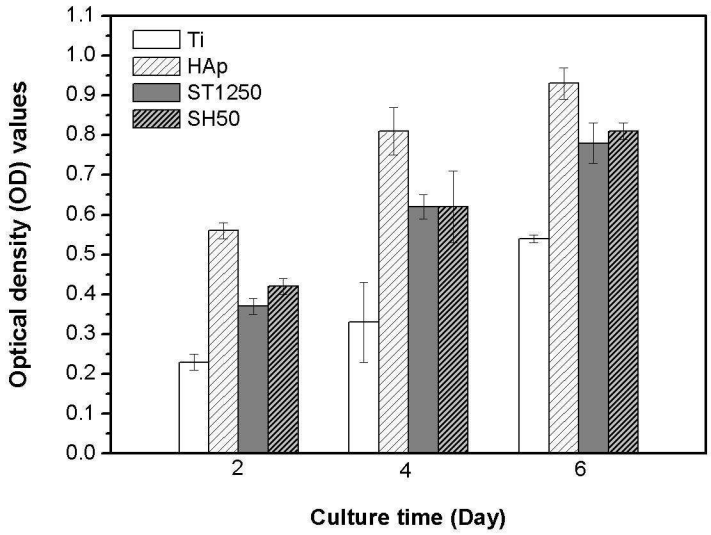

Figure 6. MTT assay of NIH3T3 cells observed on sintered HAp, SH50 and ST1250 specimens for different culture time. Titanium sample was used as a reference material.

4. Conclusions

In the present study, pure $SrTiO_3$ was synthesized from solid state reaction and the as synthesized powder and its composite ($SrTiO_3$-50%HAp) were successfully consolidated as bulk ceramic. During sintering no phase transformation happened in $SrTiO_3$ or no reaction occurred between $SrTiO_3$ and HAp. The densification of $SrTiO_3$ increased sharply at 1400 ºC. With increasing sintering temperature, hardness and elastic modulus of $SrTiO_3$ increased. The compressive strength, hardness and elastic modulus of porous $SrTiO_3$ was higher than HAp or its composite. The release of Sr^{2+} ions from porous $SrTiO_3$ increased with increasing dissolution time in PBS solution. The porous $SrTiO_3$ sample found to be biocompatible and surface was more hydrophilic compared to HAp and its composites. The cell proliferation on $SrTiO_3$ was lower than HAp but significantly higher than Ti for all the culture duration. Significantly higher compressive strength of porous $SrTiO_3$ than HAp and cytocompatibility could be useful for bone tissue engineering. Thus $SrTiO_3$ could be considered as potential biomaterial with high load bearing capability.

Acknowledgements

The authors would also like to acknowledge the financial support from the Council of Scientific and Industrial Research (CSIR), India, through project ESC 0103.

References

[1] M. Prakasam, J. Locs, K. Salma-Ancane, D. Loca, A. Largeteau, L. Berzina-Cimdina, Fabrication, properties and applications of dense hydroxyapatite: A review, J. Funct. Biomater. 6 (2015) 1099–1140.doi:10.3390/jfb6041099.

[2] A. Sáenz, E. Rivera-muñoz, W. Brostow, V.M. Castaño, Ceramic Biomaterials : an Introductory Overview, J. Mater. Educ. 21 (1999) 297–306.

[3] W. Suchanek, M. Yoshimura, Processing and Properties of HAp Based Biomaterials for Use as Hard Tissue, J. Mater. Res. 13 (2017) 94–117. doi:10.1557/JMR.1998.0015.

[4] S. Bose, S. Dasgupta, S. Tarafder, A. Bandyopadhyay, Microwave processed nanocrystalline hydroxyapatite: Simultaneous enhancement of mechanical and biological properties, Acta Biomater. 19 (2009) 389–

399.doi:10.1016/j.actbio.2010.03.016.

[5] G. Wang, S.-I. Roohani-Esfahani, W. Zhang, K. Lv, G. Yang, X. Ding, D. Zou, D. Cui, H. Zreiqat, X. Jiang, Effects of Sr-HT-Gahnite on osteogenesis and angiogenesis by adipose derived stem cells for critical-sized calvarial defect repair, Sci. Rep. 2017, 7, 41135

[6] M. Abdellahi, A. Najafinezhad, H. Ghayour, S. Saber-Samandari, A. Khandan, Preparing diopside nanoparticle scaffolds via space holder method: Simulation of the compressive strength and porosity, J Mech Behav Biomed. 72 (2017) 171-181

[7] D.Q. Pham, C.C. Berndt, U. Gbureck, H. Zreiqat, V.K. Truong, A.S.M. Ang, Mechanical and chemical properties of Baghdadite coatings manufactured by atmospheric plasma spraying, Surf Coat Tech. 378 (2019) 124945

[8] A. Khandan, N. Ozada, S. Saber-Samandari, M. Ghadiri Nejad, On the mechanical and biological properties of bredigite-magnetite ($Ca_7MgSi_4O_{16}$-Fe_3O_4) nanocomposite scaffolds. Ceram Int. 44 (2018) 3141-3148.

[9] S. Pors Nielsen, The biological role of strontium. Bone 35 (2004) 583–588.

[10] J. Li, L. Yang, X. Guo, W. Cui, S. Yang, J. Wang, Y. Qu, Z. Shao, S. Xu, Osteogenesis effects of strontium-substituted hydroxyapatite coatings on true bone ceramic surfaces in vitro and in vivo, Biomed. Mater. 13 (2018) 15018.doi:10.1088/1748-605X/aa89af.

[11] F. Yang, D. Yang, J. Tu, Q. Zheng, L. Cai, L. Wang, Strontium enhances osteogenic differentiation of mesenchymal stem cells and in vivo bone formation by activating wnt/catenin signalling, Stem Cells. 29 (2011) 981-991. doi:10.1002/stem.646.

[12] P.J. Meunier, C. Roux, E. Seeman, S. Ortolani, J.E. Badurski, T.D. Spector, J. Cannata, A. Balogh, E. M. Lemmel, S. Pors-Nielsen, R. Rizzoli, H.K. Genant, J.Y. Reginster, The Effects of Strontium Ranelate on the Risk of Vertebral Fracture in Women with Postmenopausal Osteoporosis, N. Engl. J. Med. 350 (2004) 459–468. doi:10.1056/NEJMoa022436.

[13] E. Bonnelye, A. Chabadel, F. Saltel, P. Jurdic, Dual effect of strontium ranelate: stimulation of osteoblast differentiation and inhibition of osteoclast formation and resorption in vitro. Bone 42 (2008) 129–138.

[14] P.J. Marie, Strontium as therapy for osteoporosis, Curr. Opin. Pharmacol. 5 (2005) 633–636. doi:10.1016/j.coph.2005.05.005.

[15] Kaili Lin, Lunguo Xia, Haiyan Li, Xinquan Jiang, Haobo Pan, Yuanjin Xu, William W. Lu, Zhiyuan Zhang, Jiang Chang, Enhanced osteoporotic bone regeneration by strontium-substituted calcium silicate bioactive ceramics, Biomaterials. 34 (2013) 10028-10042

[16] TH Huang, CT. Kao, YF. Shen, YT. Lin, YT. Liu, SY. Yen, CC. Ho, Substitutions of strontium in bioactive calcium silicate bone cements stimulate osteogenic

differentiation in human mesenchymal stem cells. J Mater Sci: Mater Med. 30 (2019) 68

[17] A. Pal, P. Nasker, S. Paul, A. Roy Chowdhury, A. Sinha, M. Das, Strontium doped hydroxyapatite from Mercenaria clam shells: Synthesis, mechanical and bioactivity study, J Mech Behav Biomed. 90 (2019) 328–336

[18] H.B. Pan, Z.Y. Li, W.M. Lam, J.C. Wong, B.W. Darvell, K.D.K. Luk, W.W. Lu, Solubility of strontium-substituted apatite by solid titration, Acta Biomater, 5 (2009) 1678-1685

[19] M. Frasnelli, F. Cristofaro, V.M. Sglavo, S. Dirè, E. Callone, R. Ceccato, G. Bruni, A.I. Cornaglia, L. Visai, Synthesis and characterization of strontium-substituted hydroxyapatite nanoparticles for bone regeneration, Mater. Sci. Eng. C. 71 (2017) 653–662. doi:10.1016/j.msec.2016.10.047.

[20] J.T.B. Ratnayake, M. Mucalo, G.J. Dias, Substituted hydroxyapatites for bone regeneration: A review of current trends, J. Biomed. Mater. Res. - Part B Appl. Biomater. 105 (2017) 1285–1299. doi:10.1002/jbm.b.33651.

[21] E. Gentleman, Y.C. Fredholm, G. Jell, N. Lotfibakhshaiesh, M.D. O'Donnell, R.G. Hill, M.M. Stevens, The effects of strontium-substituted bioactive glasses on osteoblasts and osteoclasts in vitro, Biomaterials. 31 (2010) 3949–3956.doi:10.1016/j.biomaterials.2010.01.121.

[22] Y. Li, Q. Li, S. Zhu, E. Luo, J. Li, G. Feng, Y. Liao, J. Hu, The effect of strontium-substituted hydroxyapatite coating on implant fixation in ovariectomized rats, Biomaterials. 31 (2010) 9006–9014. doi:10.1016/j.biomaterials.2010.07.112.

[23] W. Zhang, F. Zhao, D. Huang, X. Fu, X. Li, X. Chen, Strontium-substituted submicrometer bioactive glasses modulate macrophage responses for improved bone regeneration, Applied Materials & Interfaces. 8 (2016) 30747-30758

[24] J. Forsgren, H. Engqvist, A novel method for local administration of strontium from implant surfaces, J Mater Sci: Mater Med. 21 (2010**)** 1605–1609.doi:10.1007/s10856-010-4022-8.

[25] Y. Xin, J. Jiang, K. Huo, T. Hu, P.K. Chu, Bioactive $SrTiO_3$ nanotube arrays: strontium delivery platform on Ti-based osteoporotic bone implants, ACS Nano. 3 (2009**)** 3228–3234.doi:10.1021/nn9007675.

[26] L. Zhao, H. Wang, K. Huo, X. Zhang, W. Wang, Y. Zhang, Z. Wu, P. K. Chu, The osteogenic activity of strontium loaded titania nanotube arrays on titanium substrates, Biomaterials. 34 (2013**)** 19–29.doi:10.1016/j.biomaterials.2012.09.041.

[27] S. Sahoo, A. Sinha, V.K. Balla, M. Das, Synthesis, characterization, and bioactivity of $SrTiO_3$-incorporated titanium coating, J. Mater. Res. 33 (2018) 2087–2095. doi:10.1557/jmr.2018.99.

[28] O.Z. Andersen, V. Offermanns, M. Sillassen, K.P. Almtoft, I.H. Andersen, S.

Sørensen, C.S. Jeppesen, D.C.E. Kraft, J. Bøttiger, M. Rasse, F. Kloss, M. Foss, Accelerated bone ingrowth by local delivery of strontium from surface functionalized titanium implants, Biomaterials. 34 (2013) 5883–5890. doi:10.1016/j.biomaterials.2013.04.031.

[29] C. Capuccini, P. Torricelli, F. Sima, E. Boanini, C. Ristoscu, B. Bracci, G. Socol, M. Fini, I.N. Mihailescu, A. Bigi, Strontium-substituted hydroxyapatite coatings synthesized bypulsed-laser deposition: In vitro osteoblast and osteoclast response, Acta Biomater. 4 (2008) 1885–1893. doi:10.1016/j.actbio.2008.05.005.

[30] Y.Pai, A.Tylan-Tyler, P.Irvin, J. Levy, Physics of $SrTiO_3$-based heterostructures and nanostructures: a review, Rep Prog Phys. 81 (2018) 036503. doi:10.1088/1361-6633/aa892d.

[31] M. V. Rudenko, V. S. Kortov, N. V. Gaponenko, A. V. Mudryi, S. V. Zvonarev, Photo and cathodoluminescence of strontium titanate xerogel films doped with terbium ions, Journal of Surface Investigation. Xray, Synchrotron and Neutron Techniques. 9 (2015) 1012–1015

[32] R. Wurm, O. Dernovsek, P. Greil, Sol-Gel derived $SrTiO_3$ and $SrZrO_3$ coatings on SiC and C-fibers, J. Mater. Sci. 4 (1999) 4031–4037.doi:10.1023/A:100466801.

[33] M. Akao, H. Aoki, K. Kato, Mechanical properties of sintered hydroxyapatite for prosthetic applications, J. Mater. Sci. 16 (1981) 809–812. doi:10.1007/BF02402799.

[34] P. Nasker, A. Samanta, S. Rudra, A. Sinha, A. K. Mukhopadhyay, M. Das, Effect of fluorine substitution on sintering behaviour, mechanical and bioactivity of hydroxyapatite, J Mech Behav Biomed. 95 (2019) 136–142. doi:10.1016/j.jmbbm.2019.03.032.

[35] A.P. Sakhya, J. Maibam, S. Saha, S. Chanda, A. Dutta, B. I. Sharma, R. K. Thapa, T.P. Sinha, Electronic structure and elastic properties of $ATiO_3$ (A = Ba, Sr, Ca) perovskites: A first principles study, Indian J Pure Ap Phy. 53 (2015) 102-109

[36] R. O. Silva, J.Malzbender, F.Schulze-Küppers, S.Baumann, O.Guillon, Mechanical properties and lifetime predictions of dense SrTi1-xFexO3-δ (x = 0.25, 0.35, 0.5), J Euro Ceram Soc. 37 (2017) 2629–2636. doi:10.1016/j.jeurceramsoc.2017.02.038.

[37] A. Nakamura, K. Yasufuku, Y. Furushima, K. Toyoura, K. P. D. Lagerlöf, K. Matsunaga, Room-Temperature plastic deformation of strontium titanate crystals grown from different chemical compositions, Crystals. 7 (2017) 351. doi:10.3390/cryst7110351.

[38] K. Webb, V. Hlady, P.A. Tresco, Relative importance of surface wettability and charged functional groups on NIH 3T3 fibroblast attachment, spreading, and cytoskeletal organization, J Biomed Mater Res. 41 (1998) 422–430.

LIST OF TABLE CAPTIONS

Table 1. Density and crystallite size measurement for the bulk sintered specimens.

Table 2. Hardness, reduced elastic modulus, compressive strength and contact angle of sintered ceramics

LIST OF FIGURE CAPTIONS

Figure 1. XRD patterns of (a) HAp and as synthesized $SrTiO_3$ powder, (b) sintered samples.

Figure 2. Scanning electron micrograph of sintered specimens (a) HAp sintered at 1100 °C, (b) SH50 sintered at 1100 °C, (c) ST1250 sintered at 1250 °C, (d) ST1350 sintered at 1350 °C, and (e) ST1400 sintered at 1400 °C.

Figure 3. Vickers micro-hardness of sintered HAp, SH50, ST1250, ST1350 and ST1400 specimens.

Figure 4. Nano-indention of the bulk sintered HAp, SH50, ST1250, ST1350 and ST1400 specimens.

Figure 5. Sr^{2+} ion released from ST1250 specimen for different immersion times at the concentration of 0.1g solid per 30 ml PBS solution.

Figure 6. MTT assay of NIH3T3 cells observed on sintered HAp, SH50 and ST1250 specimens for different culture time. Titanium sample was used as a reference material.

Research Highlights

- Explored potential of $SrTiO_3$ for biomedical applications
- The hardness and compressive strength of $SrTiO_3$ found significantly higher than hydroxyapatite.
- *In vitro* cell culture showed cytocompltibility of $SrTiO_3$.

Conflicts of Interest Statement

Title: Synthesis, characterization and in vitro biocompatibility study of strontium titanate ceramic: A potential biomaterial

Authors: Souvik Sahoo, Arijit Sinha, Mitun Das

The authors have NO affiliations with or involvement in any organization or entity with any financial interest or non-financial interest in the subject matter or materials discussed in this manuscript.

Mitun Das